Precise tracking control of shape memory alloy actuator systems using hyperbolic tangential sliding mode control with time delay estimation

Article *in* Mechatronics · April 2013

DOI: 10.1016/j.mechatronics.2013.01.005

CITATIONS
36

READS
281

3 authors:

Jinoh Lee
Istituto Italiano di Tecnologia
56 PUBLICATIONS **679** CITATIONS
SEE PROFILE

Maolin Jin
Korea Institute of Robot and Convergence
73 PUBLICATIONS **907** CITATIONS
SEE PROFILE

Kyoung Kwan Ahn
University of Ulsan
296 PUBLICATIONS **3,305** CITATIONS
SEE PROFILE

Mechatronics xxx (2013) xxx–xxx

Contents lists available at SciVerse ScienceDirect

Mechatronics

journal homepage: www.elsevier.com/locate/mechatronics

Precise tracking control of shape memory alloy actuator systems using hyperbolic tangential sliding mode control with time delay estimation

Jinoh Lee [a], Maolin Jin [b], Kyoung Kwan Ahn [c,*]

[a] Department of Advanced Robotics, Istituto Italiano di Tecnologia, via Morego 30, 16163 Genoa, Italy
[b] System Solution Research Department, Research Institute of Industrial Science and Technology, Pohang 790-330, South Korea
[c] School of Mechanical Engineering, University of Ulsan, Daehakro 93, Namgu, Ulsan 680-749, South Korea

ARTICLE INFO

Article history:
Received 15 March 2012
Accepted 7 January 2013
Available online xxxx

Keywords:
Shape memory alloy actuator
Hysteresis compensation
Sliding mode control
Time delay estimation
Tracking control of SMA

ABSTRACT

This paper focuses on a simple and robust tracking control method based on a hyperbolic tangential sliding mode control (SMC) and time delay estimation (TDE) for a shape memory alloy (SMA) actuator. The TDE is used to compensate for hysteresis and other nonlinearities in the SMA dynamics, and the hyperbolic tangential SMC is used to specify nonlinear error dynamics which slides without exceeding the velocity limitation. The implementation process of the proposed control is easy by virtue of its model-free nature and transparent structure. The precise and robust tracking performance of the proposed control is verified by experiments on a bias-type SMA actuator system. Through the experiment, small tracking errors are observed throughout a significantly wide range of speed for a desired trajectory, and successfully maintained on the order of $10^{-2\circ}$ against an external disturbance.

1. Introduction

Shape memory alloys (SMAs) are metallic materials, typically made of nickel and titanium (NiTi), which have the ability to memorize a shape or size when appropriate thermal energy is applied. The shape memory effect results from a crystalline transformation between a high-temperature austenite state and a low-temperature martensite state, and the generated motion or force in this process can be used to actuate an electromechanical device by electronically heating the material. There have been various applications requiring motion control using SMAs such as artificial hands [1,2], medical equipment [3,4], automotive vehicle parts [5,6], and biomimetic robots [7,8]; these applications take advantage of SMA actuator virtues including light weight, silent operation, and high power-to-weight ratio [9].

Although many applications of SMA actuators have been developed, the tracking control of the SMA actuator is still challenging due to the highly nonlinear dynamic behavior of SMAs, that is, a *hysteresis effect* [10,11]. In order to achieve precise tracking control, one intuitive resolution is to compensate for the hysteresis using a feed-forward controller with the inverse hysteresis model of the SMA. In this sense, many literatures have proposed controls with mathematical models which are used to describe the hysteresis behavior such as the Preisach model [12–14], Duhem model [15–17], Liang model [18,19], and other empirical models [20,21]. These models impose a proportional-integral derivative (PID) control or other robust control scheme, e.g., sliding mode control (SMC) and adaptive control, as an additional feedback controller to perform position tracking. However, the aforementioned methods [12–21] need an exact mathematical model, which is difficult to obtain and requires identifying many system parameters because the dynamics of the hysteresis is highly nonlinear and complicated.

To mitigate the difficulty of obtaining the exact hysteresis model, neural network (NN)-based approaches have been incorporated in some studies. The authors in [22] proposed a tracking control with NN to reduce the hysteresis and SMC to compensate for uncertainties. Another group [23] developed a motion controller which uses a dynamic model generated by a neuro-fuzzy inference system and a proportional-derivative feedback controller. In [11], the NN is used to learn the inverse model of the hysteresis, and a proportional-integral control with anti-windup is applied together. The use of NN-based approaches, however, requires determination of a number of parameters (e.g., 33 weighting parameters used in [22], 512 in [23], and 320 in [11]), which have to be calculated through an off-line training process with an elaborate learning algorithm. Thus, NN-based control is not easy to implement for SMA actuators.

From the point-of-view of practicing engineers, a preferred controller is one that is robust and highly accurate, but is less complex [24]. Hence, we introduce a *time delay estimation* (TDE) method [25–27] without complicated modeling to compensate for nonlinearities including the hysteresis effect, which is the main difficulty

* Corresponding author.
E-mail address: kkahn@ulsan.ac.kr (K.K. Ahn).

0957-4158/$ - see front matter © 2013 Elsevier Ltd. All rights reserved.
http://dx.doi.org/10.1016/j.mechatronics.2013.01.005

associated with controlling SMA actuator systems. The core principle of the TDE is to estimate unknown dynamics and disturbances by using the input–output relationship of the closed-loop system with *intentionally* time-delayed information. In this paper, we propose a tracking controller for the SMA actuator system which consists of a combination of SMC and TDE. SMC is one popular robust control strategy that has two steps in the design process. The first step is defining a reaching phase to force the systems trajectory to reach a stable manifold, and the second step involves designing a sliding surface that assures the desired error dynamics of the closed-loop system. In this study, a nonlinear sliding surface with hyperbolic tangent function is defined in attempt to alleviate the negative effects resulting from velocity saturation of the SMA actuator and noise due to numerical differentiation. Using the combination of SMC with a hyperbolic tangential sliding surface and the TDE, we propose a simple, model-free, accurate, but robust controller.

The contribution we attempt to make is as follows. The first is to propose a precise tracking control method for the SMA actuation system combining SMC with a nonlinear sliding surface and the TDE; and the second is to validate the simplicity, high accuracy and robustness of the proposed control using physical experiments.

This paper is organized as follows Section 2 proposes a tracking control method, i.e., SMC with a hyperbolic tangential sliding surface and TDE, and discusses the properties of the control. In Section 3, the experimental setup of the SMA actuator system is explained, and several experiments are performed to verify the highly accurate tracking performance and robustness of the proposed control. Finally, the conclusions are presented in Section 4.

2. Proposed control law for SMA

2.1. Problem definition of tracking control for the SMA actuator system

The SMA actuator system is shown in Fig. 1. We consider the linear motion of the bias-type actuator. There have been many works on the dynamic model of the SMA actuator [12–21]. In this paper, we used the following second-order dynamics of the SMA actuator system, which is obtained from [17,28,29]:

$$J\ddot{\theta} + b\dot{\theta} + k\theta + d = h(\theta, \dot{\theta}, u) + \alpha u, \tag{1}$$

where $\theta, \dot{\theta}$, and $\ddot{\theta}$ represent the angular position, the velocity and the acceleration of the system, respectively, J, b, and k denote an effective inertia, an effective damping, and an effective stiffness, respectively, while d expresses unexpected disturbances, $h(\theta, \dot{\theta}, u)$ is the hysteretic nonlinear term, u is the applied current, and α is the input coefficient.

The target of the control is to allow the position of the actuator, θ, to track the desired trajectory, θ_d. The tracking error between the actual position and the desired position is defined as

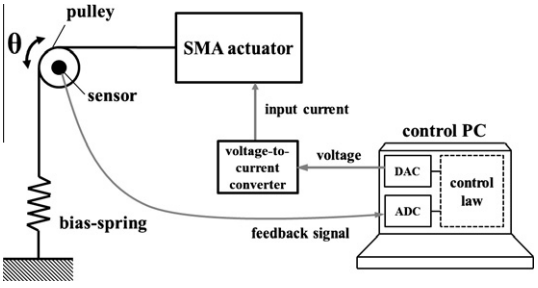

Fig. 1. The schematic diagram of an SMA actuator system.

$$e \triangleq \theta_d - \theta. \tag{2}$$

2.2. Proposed SMC with a nonlinear sliding surface using TDE

The SMA actuator dynamics, (1), can be reformulated by introducing a constant $\bar{m}$ as follows:

$$\bar{m}\ddot{\theta} + \eta(\theta, \dot{\theta}, \ddot{\theta}, u) = u, \tag{3}$$

where

$$\eta(\theta, \dot{\theta}, \ddot{\theta}, u) = (J/\alpha - \bar{m})\ddot{\theta} + [b\dot{\theta} + k\theta + d - h(\theta, \dot{\theta}, u)]/\alpha \tag{4}$$

represent all the nonlinearities of the SMA actuator system including the hysteresis effect and external disturbances.

Here, a nonlinear sliding surface with a hyperbolic tangent function (tanh) is defined as

$$s = \dot{e} + \lambda_1 \tanh(ke), \tag{5}$$

where k is a positive constant value which is related to the slope of tanh, and λ_1 denotes a design value which is determined by considering the velocity limit of the SMA actuator. The above sliding surface is designed in order to attenuate the unfavorable effects of large velocity error in the SMA actuator system. The physical meaning of the nonlinear sliding surface with tanh is further discussed in Section 2.3.1.

The hyperbolic tangential sliding surface, (5), is continuous and differentiable; hence its first derivative can be expressed as

$$\dot{s} = \ddot{e} + \lambda_1 \frac{k}{\cosh^2(ke)}\dot{e}. \tag{6}$$

A dynamic attractor of the reaching phase is chosen as

$$\dot{s} + \lambda_2 s = 0, \tag{7}$$

where λ_2 denotes a design value. From (5)–(7), the desired closed-loop error dynamics for the tracking control is then derived as follows:

$$\ddot{e} + \left(\lambda_1 \frac{k}{\cosh^2(ke)} + \lambda_2\right)\dot{e} + \lambda_1\lambda_2 \tanh(ke) = 0. \tag{8}$$

In order to achieve the above mentioned closed-loop error dynamics, the control input can be selected as

$$u = \bar{m}v + \hat{\eta}, \tag{9}$$

where

$$v = \ddot{\theta}_d + \left(\lambda_1 \frac{k}{\cosh^2(ke)} + \lambda_2\right)\dot{e} + \lambda_1\lambda_2 \tanh(ke) \tag{10}$$

and $\hat{\eta}$ denotes the estimated value of the nonlinearities, $\eta(\theta, \dot{\theta}, \ddot{\theta}, u)$.

The aforementioned SMC attempts to cancel $\eta(\theta, \dot{\theta}, \ddot{\theta}, u)$ in (4) by the estimated value of the nonlinearity, $\hat{\eta}$, and forces the error behavior of the closed-loop system to lie along a chosen sliding manifold without chattering. However, in (9), $\hat{\eta}$ is difficult to obtain because it contains not only complex hysteresis behavior, but also external disturbances. Therefore, the proposed control incorporates the TDE [25–27], which enables simple and effective estimation of the nonlinearity of the SMA actuator system.

The TDE performs *indirect* estimates on the basis of the continuity of the SMA dynamics (1), that is, the following holds:

$$\lim_{L\to 0}\eta(\theta, \dot{\theta}, \ddot{\theta}, u)_{(t-L)} = \eta(\theta, \dot{\theta}, \ddot{\theta}, u)_{(t)}, \tag{11}$$

where L denotes the time delay, and $\bullet_{(t-L)}$ is the value of $\bullet$ at the delayed time $(t - L)$. Hence, $\eta(\theta, \dot{\theta}, \ddot{\theta}, u)_{(t-L)}$ may be used as a good estimate for $\eta(\theta, \dot{\theta}, \ddot{\theta}, u)$, provided that L is sufficiently small [25–27,30,31]. That is,

Please cite this article in press as: Lee J et al. Precise tracking control of shape memory alloy actuator systems using hyperbolic tangential sliding mode control with time delay estimation. Mechatronics (2013), http://dx.doi.org/10.1016/j.mechatronics.2013.01.005

$$\hat{\eta} = \eta(\theta, \dot{\theta}, \ddot{\theta}, u)_{(t-L)}. \tag{12}$$

From (3) and (12), the TDE can be derived as follows:

$$\hat{\eta} = \eta(\theta, \dot{\theta}, \ddot{\theta}, u)_{(t-L)} = u_{(t-L)} - \bar{m}\ddot{\theta}_{(t-L)}. \tag{13}$$

Finally, by combination of (9), (10) and (13), the hyperbolic tangential SMC with TDE is expressed as follows:

$$u = \underbrace{\bar{m}[\ddot{\theta}_d + (\lambda_1 k \cosh^{-2}(ke) + \lambda_2)\dot{e} + \lambda_1\lambda_2 \tanh(ke)]}_{\text{SMC with the nonlinear sliding surface}} + \underbrace{u_{(t-L)} - \bar{m}\ddot{\theta}_{(t-L)}}_{\text{TDE for compensating hysteresis and other nonlinearities}} \tag{14}$$

As seen in the above equation, the proposed controller has a transparent structure. That is, the SMC leads the SMA actuator system to accurately and robustly follow a desired trajectory, while the TDE simply compensates for nonlinearities of the SMA actuator system, especially the hysteresis behavior, without a mathematical model. In the controller, $\bar{m}$ is a control gain which is usually tuned, λ_1 is a control parameter selected by considering the velocity limit of the actuator, while k and λ_2 are control parameters for determining the dynamics of the sliding phase and reaching phase, respectively.

Note that, sufficiently small L is crucial for the TDE to function correctly in the proposed control. Since the control is implemented on a digital device, the smallest achievable L becomes the sampling period of the controller. The authors in [32] refer that a digital control system can be regarded as a continuous system when the sampling period is sufficiently fast, more specifically, 30 times faster than the system bandwidth. Thus, the TDE shown in (12) is valid. In the experiment described below, we used a 1 ms sampling period.

The stability proof of the proposed control is provided in the Appendix.

2.3. Properties of proposed control

2.3.1. Characteristics of error dynamics

The SMA actuator has small displacement and a relatively slow response speed due to the cooling phase [33,34]. Considering the intrinsic slow response of the target system, we designed a hyperbolic tangential sliding surface, as shown in (5). This subsection investigates the error dynamics relating to the physical meaning of the hyperbolic tangential sliding surface.

Illustrated in Fig. 2 are the phase portraits of the closed-loop error dynamics both with a linear and a hyperbolic tangential sliding surface. When error occurred in the closed-loop system, the dynamic attractor, (7), forces the states of the system to exponentially converge to the sliding surface. Once the system trajectory reaches the sliding surface $s(t) = 0$, it moves along the sliding surface to the origin, corresponding to the dynamics form of the sliding mode. Shown in Fig. 2a is the hyperbolic tangential sliding mode, (5), in the case of $\lambda_1 = 10$ and $k = 1$. If the error is a small distance from the zero point, the system trajectory goes to zero with a high convergence rate, which is determined by k; when a large error occurs, the hyperbolic tangential sliding mode *prevents the velocity error from exceeding the limit* determined by λ_1. Whereas, if the system trajectory moves along the linear sliding mode, $s = \dot{e} + 10e = 0$, as shown in Fig. 2b, a large velocity error appears, and the velocity error $(\dot{e})$ becomes much worse as the error (e) becomes large.

The large velocity error may cause velocity saturation since the maximum velocity of the actuator is physically limited in real applications. According to [35–37], the presence of the velocity saturation of actuators severely effects the tracking control performance, e.g., an excessive overshoot. Additionally, as the velocity error becomes larger, the controller can be further affected by negative effects due to the numerical differentiation because the velocity is calculated by the numerical differentiation, which generally amplifies quantization error and sensor noise.

As previously mentioned, the hyperbolic tangential sliding surface, (5), enables the closed-loop system to simply and effectively avoid the large velocity error of the tracking control; therefore, it can be a good alternative from the perspective of velocity saturation of the SMA actuator and the use of velocity information calculated via numerical differentiation.

2.3.2. Simplicity of the control

The proposed control uses the TDE in order to compensate for the nonlinearities of the SMA actuator system including hysteresis and unmodeled dynamics, such as friction; that is, the TDE makes the proposed control *simple* and *model-free*.

In (13), the TDE is calculated using time-delayed values of the control input and the acceleration. These time-delayed values are simply obtained by *storing* the values of the previous step in the buffer memory of the controller, and the acceleration $\ddot{\theta}_{(t-L)}$ can be calculated by brief numerical differentiation, $\ddot{\theta}_{(t-L)} = (\theta_{(t)} - 2\theta_{(t-L)} + \theta_{(t-2L)})L^{-2}$. Furthermore, the proposed control has only a few control parameters, as shown in Table 1. Thus, its implementation process

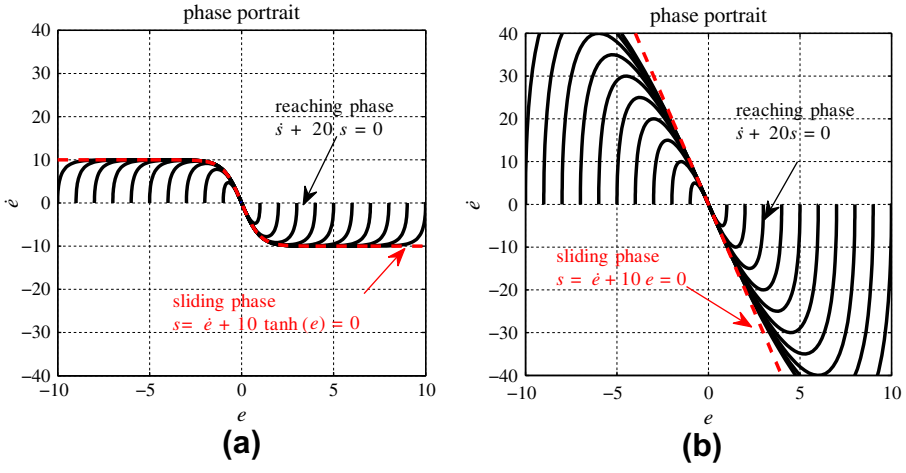

Fig. 2. The phase portrait of closed-loop error dynamics: (a) with the hyperbolic tangential sliding surface and (b) with a linear sliding surface.

Please cite this article in press as: Lee J et al. Precise tracking control of shape memory alloy actuator systems using hyperbolic tangential sliding mode control with time delay estimation. Mechatronics (2013), http://dx.doi.org/10.1016/j.mechatronics.2013.01.005

Table 1
Comparisons of control parameters.

	For hysteresis compensation	For tracking desired trajectory
SMC with NN [22]	33 Weights for learning	2 Tuning gains, 4 design parameters
PD control with neuro-fuzzy [23]	512 Weights for learning	2 Tuning gains
PI control with NN [11]	340 Weights for learning	2 Tuning gains
Proposed control	1 Tuning gain	3 Design parameters

including the gain tuning is particularly easy. As we discussed in the previous subsections, λ_1 is a design parameter selected by considering the velocity limit of the actuator; k and λ_2 are also determined by the designer's choice relating to the convergence speed of the sliding phase and reaching phase, respectively. Therefore, $\bar{m}$ is the only gain to be tuned in the proposed control. The value of $\bar{m}$ is chosen analytically by J/α from the relationships in (3) and (4); however, the exact value of J/α is difficult to obtain practically. Hence, it is preferable to tune $\bar{m}$ by *gradually increasing from a small positive value* just before the response of the closed-loop system becomes noisy.

Incidentally, it is worthwhile to discuss the noise effect due to the numerical differentiation because the use of TDE costs acceleration information for the simple dynamics compensation. The calculation of the acceleration via numerical differentiation is easily corrupted by the noise of the sensor signal, thus a low-pass filter (LPF) is required to attenuate the noise effect. Fortunately, lowering $\bar{m}$, the controller gain, has the same effect as using a first-order digital LPF [38,31]. Hence, the effect of attenuating the noise is incorporated in the above mentioned tuning process of $\bar{m}$. Since there is no need to use an additional LPF against the noise of numerical differentiation, the implementation of the proposed control is simplified.

3. Experimental verification

This section experimentally validates the effectiveness and the robustness of the proposed hyperbolic tangential SMC with TDE for the SMA actuator system.

3.1. Experimental setup

As shown in Fig. 3, the SMA actuator system consists of a NiTi type SMA actuator with a bias-spring, DM01, which is manufactured by MIGA Motor Company with the following specifications: the linear stroke is 16 mm and the generated force is 20 N. A high precision potentiometer, Copal JT30, measures the displacement of the SMA actuator. The analog feedback signal of the sensor is converted into a digital signal by a 14-bit ADC of Sensoray S626—a multi-functional data acquisition (DAQ) board. The resolution of the sensor is determined by the ADC as 0.0183°, and the root-mean-squared (RMS) value of the measurement noise is 0.01° after applying a first-order digital LPF to the sensor signal, as shown in Fig. 4. The aforementioned DAQ board also has 13-bit DACs and thus generates an analog voltage for the control input.

Note that, since the proposed controller is designed for the current control of an SMA actuator, the analog voltage is transformed into current by a V/I convertor, Lord RD-3002-1, with a voltage-to-current ratio of 0.4 A/V and a current limit of 2 A. The controller is digitally implemented using C++ language under a real-time operating system QNX 4 with a 2.4 GHz CPU mounted on an industrial PC.

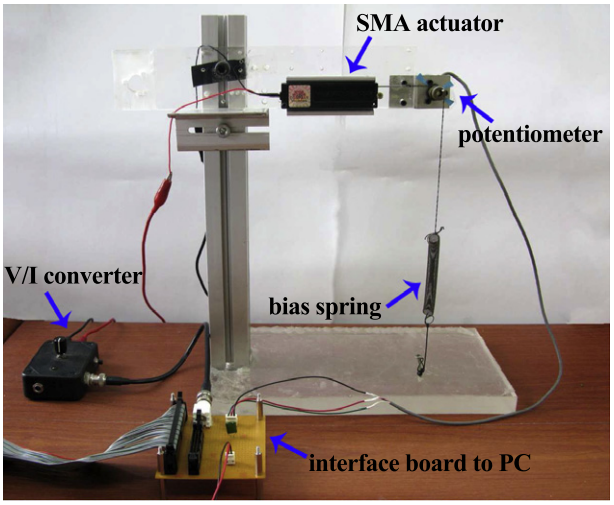

Fig. 3. Experimental setup of the SMA actuator system.

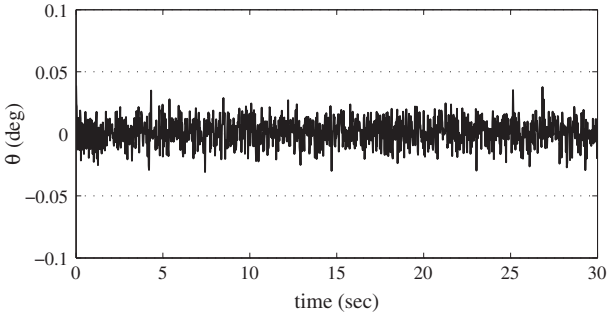

Fig. 4. The feedback signal of potentiometer.

3.2. Controller settings

The control parameters of the proposed controller, as shown in (14), are selected as $\lambda_1 = \lambda_2 = 8.0$ and $k = 1.0$, and the gain $\bar{m}$ is tuned to 0.001. Derivatives $\dot{\theta}$ and $\ddot{\theta}_{(t-L)}$ are obtained by the numerical differentiation with the backward difference. The sampling period is set to 1 ms; thus, $L = 1$ ms. Note that, as previously mentioned, the noise effect of the acceleration due to numerical differentiation is attenuated by lowering $\bar{m}$, which is a part of the gain tuning process.

To validate the tracking control performance, the SMA actuator is commanded by desired trajectories of the fifth-order polynomial, as shown in Fig. 5. The low-speed trajectory has a 1.25°/s maximum velocity, mid-speed trajectory has a 3.75°/s maximum velocity, and the high-speed trajectory has a 12.5°/s maximum velocity.

The effectiveness of the proposed controller is demonstrated by experimental comparisons to PID control, which has the following form:

$$u = K_P e + K_D \dot{e} + K_I \int (e \, \mathrm{d}t). \tag{15}$$

For a fair comparison, three gains of PID control are tuned by the particle swarm optimization (PSO) method [17]. An objective function chosen for the PSO is mean-square error between a reference command and an actual response. The optimized PID gains are obtained after 100 iterations of tunning so that it minimizes the objective function; and the results from the PSO are $K_P = 9.92$, $K_D = 0.3987$, and $K_I = 0.3947$.

Please cite this article in press as: Lee J et al. Precise tracking control of shape memory alloy actuator systems using hyperbolic tangential sliding mode control with time delay estimation. Mechatronics (2013), http://dx.doi.org/10.1016/j.mechatronics.2013.01.005

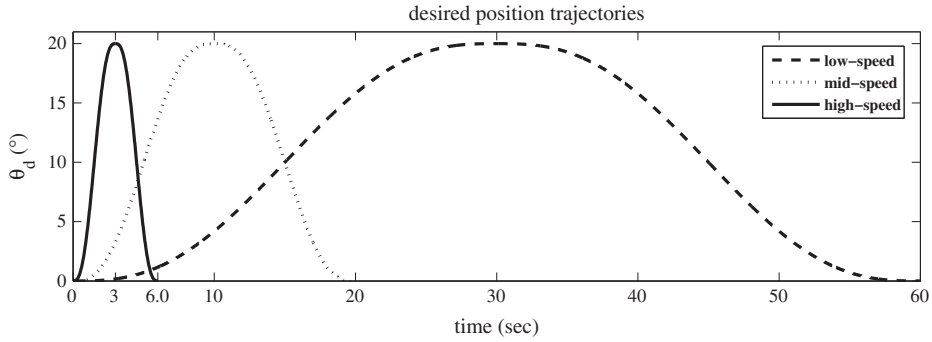

Fig. 5. The desired trajectories for the tracking control: The broken line indicates the low-speed trajectory, t = 0–60 s; the dotted line indicates the mid-speed trajectory, t = 0–20 s; and the solid line indicates the high-speed trajectory, t = 0–6 s.

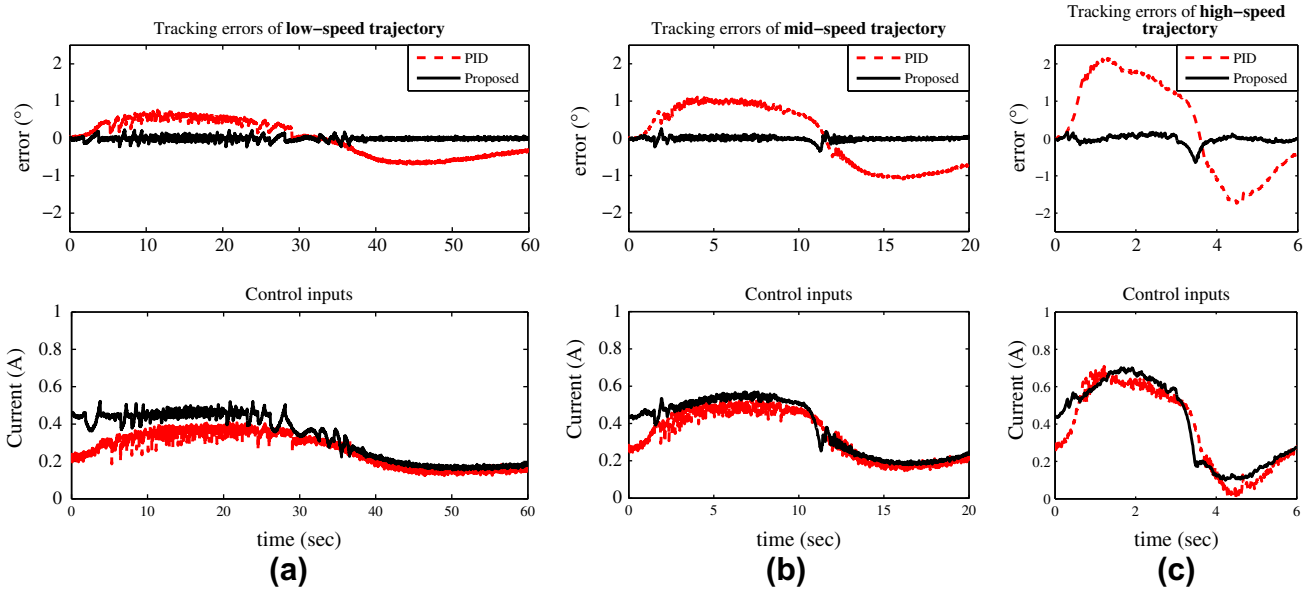

Fig. 6. The error responses and the control inputs: (a) for the low-speed trajectory; (b) for the mid-speed trajectory and (c) for the high-speed trajectory. The red broken line indicates the result of PID control and the black solid line indicates that of proposed control. (For interpretation of the references to colour in this figure legend, the reader is referred to the web version of this article.)

3.3. Results

The experimental results are shown in Fig. 6, and Tables 2 and 3. The error responses in Fig. 6 indicate that the proposed control enables the SMA actuator to precisely follow the desired trajectory and achieve a smaller tracking error than PID control with optimized gains. Although the error response of both controllers gets worse as the speed of the desired trajectory goes faster, the proposed control performs much better than PID control; when low- and high-speed cases are compared, the maximum error of PID control increases by 1.4383° whereas that of proposed control increases by 0.4119°. As shown in Tables 2 and 3, RMS error values of proposed control are 8–12% of those of PID control, and its maximum error values are 29–31% of those of PID control for low-, mid- and high-speed trajectories. The control inputs, shown in Fig. 6, reveal that the sliding mode of the proposed control operates without significant control chatter.

Table 2
RMS values of tracking error (°).

	Low speed	Mid speed	High speed
PID	0.4661	0.8168	1.3712
Proposed	0.0573	0.0677	0.1299

Table 3
Maximum tracking errors (°).

	Low speed	Mid speed	High speed
PID	0.7597	1.1052	2.1980
Proposed	0.2356	0.3468	0.6475

In addition, the hysteresis curve of the closed-loop system is shown in Fig. 7. While the hysteresis effect remains when using PID control with optimized gains, the SMA actuator system is almost linearized by using the proposed control. This result verifies that the proposed control can simply and effectively compensate the nonlinear effect of hysteresis without a model thanks to TDE.

In order to verify the robustness of the proposed control, an additional load is applied by adjusting the number of winding threads attached to the bias spring, as shown in Fig. 8. The additional load acts as an external disturbance, and the amount of added load is added by 118% to that of the previous experiment

Please cite this article in press as: Lee J et al. Precise tracking control of shape memory alloy actuator systems using hyperbolic tangential sliding mode control with time delay estimation. Mechatronics (2013), http://dx.doi.org/10.1016/j.mechatronics.2013.01.005

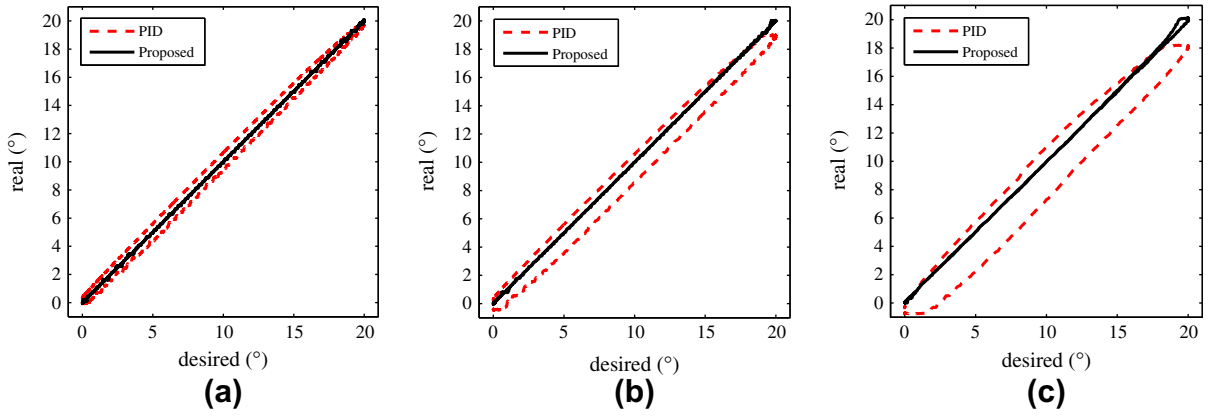

Fig. 7. Hysteresis curves of SMA actuator system after applying controls: (a) at the low-speed trajectory; (b) at the mid-speed trajectory and (c) at the high-speed trajectory.

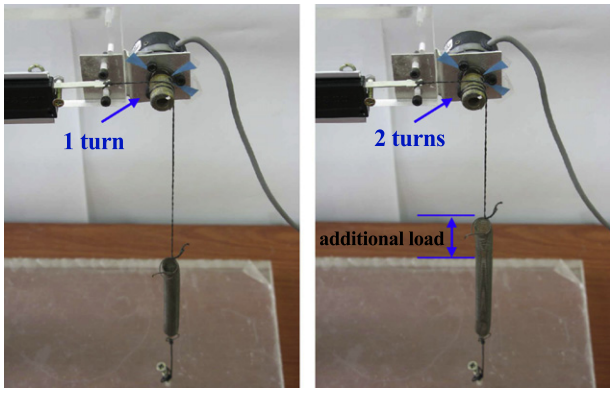

Fig. 8. Change of the setting to add a load as an external disturbance (right).

setup. Note that the change in loading conditions also affects the hysteresis of the system [22]. In the following experiment, the same parameters for the proposed controller are used to compare the control performance before and after adding the load, and a mid-speed desired trajectory, shown in Fig. 5a, is used for both experiments.

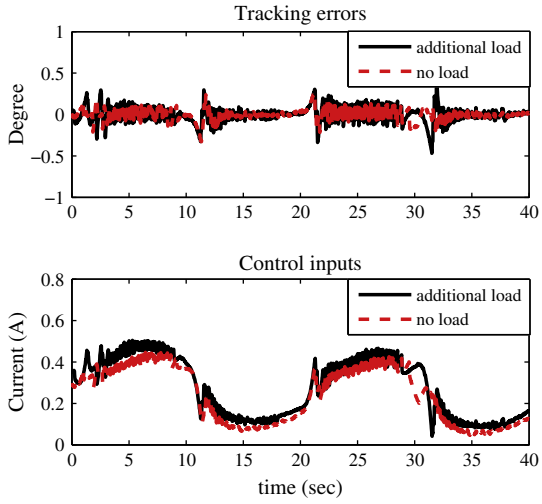

Fig. 9. The error responses and the control inputs for the mid-speed trajectory: the red broken line indicates the result without the additional load and the black solid line indicates that with the additional load. (For interpretation of the references to colour in this figure legend, the reader is referred to the web version of this article.)

Table 4
RMS values of tracking error (°).

No load	0.0680
Additional load	0.0877

The experimental results are shown in Fig. 9 and Table 4. Regardless of the external disturbance load, the proposed control shows very accurate tracking performance. The tracking error slightly increases with load, but this small difference is within the level of the sensor resolution. The control input is increased in order to compensate for the external load, which is approximately 0.0364 A.

In summary, the proposed hyperbolic tangential SMC with TDE shows that precise tracking control performance can be achieved on the order of 10^{-2} °, and the nonlinear hysteresis is simply but effectively compensated without a model due to the TDE. The robustness of the proposed control is also verified through the experiment.

4. Conclusions

In line with the practicing engineer's need for control of SMA actuator systems, simple but accurate tracking control is proposed by the combination of SMC with a hyperbolic tangential sliding surface and a TDE. The hyperbolic tangential sliding surface yields accurate and chatter-free control, and the TDE provides simplicity and robustness to the controller in spite of the hysteresis effect of the SMA. In addition, the clear structure of the controller helps user to implement this control concept in a straightforward manner.

The proposed control is physically implemented to control a bias-type SMA actuator system. Experimental verification confirms that the proposed controller was able to precisely track the desired trajectories through a significantly wide range of speed and showed better results than that of a PID control with optimized gains. Furthermore, the highly accurate tracking performance was maintained against unexpected disturbances.

Appendix A. Stability analysis

By substituting the control input, (9), into the dynamic Eq. (3), the closed-loop dynamics due to the proposed control becomes

$$\bar{m}(v - \ddot{\theta}) = \eta - \hat{\eta}. \tag{A.1}$$

Please cite this article in press as: Lee J et al. Precise tracking control of shape memory alloy actuator systems using hyperbolic tangential sliding mode control with time delay estimation. Mechatronics (2013), http://dx.doi.org/10.1016/j.mechatronics.2013.01.005

When we define the TDE error ϵ as

$$\epsilon \triangleq \bar{m}^{-1}(\eta - \hat{\eta}), \tag{A.2}$$

Eq. (A.1) is rearranged as follows:

$$v - \ddot{\theta} = \epsilon. \tag{A.3}$$

From (5), (10), and (A.3), the closed-loop dynamics can be obtained as follows:

$$\dot{s} + \lambda_2 s = \epsilon. \tag{A.4}$$

(A.4) indicates that if ϵ is asymptotically bounded, then the overall system is bounded-input-bounded-output (BIBO) stable. Hence, the asymptotic boundedness of ϵ should be investigated to analyze the closed-loop system stability. In this paper, the boundedness of ϵ is proved by the same method of the stability proof in [39,40].

Substituting (A.3) to (1), the dynamics equation of the SMA system can be expressed as

$$J\epsilon = Jv + \xi - \alpha u, \tag{A.5}$$

where $\xi \triangleq b\dot{\theta} + k\theta + d - h(\theta, \dot{\theta}, u)$. By combination of (9) and (A.5), the closed-loop system is represented as follows:

$$J\epsilon = (J - \alpha\bar{m})v + \xi - \alpha\hat{\eta}. \tag{A.6}$$

From (3) and (12), (A.6) is expressed as follows:

$$\begin{aligned} J\epsilon &= (J - \alpha\bar{m})v + \xi - (J_{(t-L)} - \alpha\bar{m})\ddot{\theta}_{(t-L)} - \xi_{(t-L)} \\ &= (J - \alpha\bar{m})v - (J_{(t-L)} - \alpha\bar{m})\ddot{\theta}_{(t-L)} + \psi, \end{aligned} \tag{A.7}$$

where

$$\begin{aligned} \psi &\triangleq \xi - \xi_{(t-L)} \\ &= b\dot{\theta} + k\theta + d - h(\theta, \dot{\theta}, u) - b\dot{\theta}_{(t-L)} - k\theta_{(t-L)} - d_{(t-L)} + h(\theta, \dot{\theta}, u)_{(t-L)}. \end{aligned} \tag{A.8}$$

Note that the hysteresis term $h(\theta, \dot{\theta}, u)$ shown in (A.8) is a non-smooth nonlinearity, but a Lipschitz-continuous function because it is well known that many hysteresis operators are Lipschitz continuous [41–44]; the unexpected discontinuous term d can be divided as $d = d_{sm} + d_{dis}$, where d_{sm} is smooth, that is, continuous and differentiable, while d_{dis} is discontinuous and assumed to be bounded. Then, we can divide ψ into smooth, Lipschitz-continuous, and discontinuous terms as follows:

$$\psi = \psi_{sm} + \psi_{Lip} + \psi_{dis}, \tag{A.9}$$

where

$$\psi_{sm} = b\dot{\theta} + k\theta + d_{sm} - b\dot{\theta}_{(t-L)} - k\theta_{(t-L)} - d_{sm(t-L)}, \tag{A.10}$$

$$\psi_{Lip} = -h(\theta, \dot{\theta}, u) + h(\theta, \dot{\theta}, u)_{(t-L)}, \tag{A.11}$$

$$\psi_{dis} = d_{dis} - d_{dis(t-L)}. \tag{A.12}$$

If the boundedness and smoothness condition of $b\dot{\theta} + k\theta + d_{sm}$ are satisfied, $\psi_{sm} = O(L^2)$ as shown in [45]. From the Lipschitz-continuous condition [46], we can obtain that $\psi_{Lip} = O(L)$. In addition, it is clear that $|\psi_{dis}| \leqslant \beta$, where β is a positive constant value. Therefore, ψ is bounded by $|\psi| \leqslant \beta + O(L)$ for a sufficiently small L. And, the approximation error can become small by reducing the sampling period.

Substituting $\ddot{\theta}_{(t-L)} = v_{(t-L)} - \epsilon_{(t-L)}$ from (A.3) into (A.7) gives

$$J\epsilon = (J - \alpha\bar{m})v - (J - \alpha\bar{m})(v_{(t-L)} - \epsilon_{(t-L)}) - (J_{(t-L)} - J)\ddot{\theta}_{(t-L)} + \psi. \tag{A.13}$$

Eq. (A.13) can be rearranged as

$$\epsilon = [1 - (\alpha\bar{m}/J)]\epsilon_{(t-L)} + [1 - (\alpha\bar{m}/J)]\kappa_1 + \kappa_2, \tag{A.14}$$

where $\kappa_1 = v - v_{(t-L)}$ and $\kappa_2 = [(J - J_{(t-L)})\ddot{\theta}_{(t-L)} + \psi]/J$.

Then, (A.14) can be expressed in the discrete-time domain as follows:

$$\epsilon_{(k)} = [1 - \alpha\bar{m}/J_{(k)}]\epsilon_{(k-1)} + [1 - \alpha\bar{m}/J_{(k)}]\kappa_{1(k)} + \kappa_{2(k)}, \tag{A.15}$$

with $\kappa_{1(k)} = v_{(k)} - v_{(k-1)}$ and $\kappa_{2(k)} = [(J_{(k)} - J_{(k-1)})\ddot{\theta}_{(k-1)} + \psi_{(k)}]/J_{(k)}$ where $\bullet_{(k)}$ denotes the $\bullet$ of the kth sampling instant. Because $\kappa_1(k)$ and $\kappa_2(k)$, forcing functions of ϵ (k), are bounded for a sufficiently small time-delay L, the first-order differential equation shown in (A.15) is asymptotically bounded if the roots of $[1 - \alpha\bar{m}/J_{(k)}]$ reside inside a unit circle as

$$|\epsilon| \leqslant \gamma, \tag{A.16}$$

where γ is a positive value.

From (A.4) and (A.16), we can finally obtain the following inequality equation:

$$|\dot{s} + \lambda_2 s| \leqslant \gamma. \tag{A.17}$$

Then, Lyapunov-based stability of the overall system can be proved. When the Lyapunov function is taken as $V = 0.5s^2$, the derivative of V is given by $\dot{V} = -\lambda_2 s^2 + s\epsilon$. Thus, we can obtain $\dot{V} < 0$ under the condition $|s| > \lambda_2^{-1}\gamma$. Since the ϵ is bounded, s is globally uniformly ultimately bounded with the ultimate bound $|s| \leqslant \lambda_2^{-1}\gamma$.

References

[1] Price AD, Jnifene A, Naguib HE. Design and control of a shape memory alloy based dexterous robot hand. Smart Mater Struct 2007;16(4):1401–14.
[2] Ko J, Jun MB, Gilardi G, Haslam E, Park EJ. Fuzzy pwm-pid control of cocontracting antagonistic shape memory alloy muscle pairs in an artificial finger. Mechatronics 2011;21(7):1190–202.
[3] Kode V, Cavusoglu M. Design and characterization of a novel hybrid actuator using shape memory alloy and dc micromotor for minimally invasive surgery applications. Mechatronics, IEEE/ASME Trans 2007;12(4):455–64.
[4] Ho M, McMillan AB, Simard JM, Gullapalli R, Desai JP. Toward a meso-scale sma-actuated mri-compatible neurosurgical robot. Robotics, IEE Trans 2012;28(1):213–22.
[5] Dayananda G, Varughese B, Subba Rao M. Shape memory alloy based smart landing gear for an airship. J Aircr 2007;44(5):1469–77.
[6] Williams EA, Shaw G, Elahinia M. Control of an automotive shape memory alloy mirror actuator. Mechatronics 2010;20(5):527–34.
[7] Saito T, Kagiwada T, Harada H. Development of an earthworm robot with a shape memory alloy and braided tube. Adv Robotic 2009;23(12-13):1743–60.
[8] Yuk H, Kim D, Lee H, Jo S, Shin JH. Shape memory alloy-based small crawling robots inspired by c. elegans. Bioinsp Biomim 2011;6(4):046002. pages 10.
[9] Nespoli A, Besseghini S, Pittaccio S, Villa E, Viscuso S. The high potential of shape memory alloys in developing miniature mechanical devices: A review on shape memory alloy mini-actuators. Sen Actuat A: Phys 2010;158(1):149–60.
[10] Lagoudas D. Shape memory alloys: modeling and engineering applications. Springer Verlag; 2008.
[11] Asua E, Etxebarria V, Garcia-Arribas A. Neural network-based micropositioning control of smart shape memory alloy actuators. Eng Appl Artif Int 2008;21(5):796–804.
[12] Majima S, Kodama K, Hasegawa T. Modeling of shape memory alloy actuator and tracking control system with the model. Control Syst Technol, IEEE Trans 2001;9(1):54–9.
[13] Ahn KK, Kha NB. Modeling and control of shape memory alloy actuators using preisach model, genetic algorithm and fuzzy logic. Mechatronics 2008;18(3):141–52.
[14] Nguyen BK, Ahn K. Feedforward control of shape memory alloy actuators using fuzzy-based inverse preisach model. Con Syst Technol, IEEE Trans 2009;17(2):434–41.
[15] Briggs J, Ostrowski J. Experimental feedforward and feedback control of a one-dimensional sma composite. Smart Mater Struct 2002;11(1):9–23.
[16] Liu SH, Huang TS, Yen JY. Tracking control of shape-memory-alloy actuators based on self-sensing feedback and inverse hysteresis compensation. Sensors 2009;10(1):112–27.
[17] Tai N, Ahn K. Adaptive proportional–integral–derivative tuning sliding mode control for a shape memory alloy actuator. Smart Mater Struct 2011;20(5):1–13.
[18] Elahinia MH, Ashrafiuon H. Nonlinear control of a shape memory alloy actuated manipulator. J Vib Acoust 2002;124(4):566–75.
[19] Gilardi G, Haslam E, Bundhoo V, Park EJ. A shape memory alloy based tendon-driven actuation system for biomimetic artificial fingers, Part II: Modelling and control. Robotica 2010;28(5):675–87.

Please cite this article in press as: Lee J et al. Precise tracking control of shape memory alloy actuator systems using hyperbolic tangential sliding mode control with time delay estimation. Mechatronics (2013), http://dx.doi.org/10.1016/j.mechatronics.2013.01.005

[20] Jayender J, Patel R, Nikumb S, Ostojic M. Modeling and control of shape memory alloy actuators. Control Syst Technol, IEEE Trans 2008;16(2):279–87.
[21] Romano R, Tannuri EA. Modeling, control and experimental validation of a novel actuator based on shape memory alloys. Mechatronics 2009;19(7):1169–77.
[22] Song G, Chaudhry V, Batur C. Precision tracking control of shape memory alloy actuators using neural networks and a sliding-mode based robust controller. Smart Mater Struct 2003;12:223–31.
[23] Kumagai A, Liu TI, Hozian P. Control of shape memory alloy actuators with a neuro-fuzzy feedforward model element. J Int Manuf 2006;17:45–56.
[24] Anderson B. Controller design: moving from theory to practice. Control Syst, IEEE 1993;13(4):16–25.
[25] Morgan R, Ozguner U. A decentralized variable structure control algorithm for robotic manipulators. Robot Automat, IEEE J 1985;1(1):57–65.
[26] Hsia T. A new technique for robust control of servo systems. IEEE Trans Ind Electron 1989;36(1):1–7.
[27] Youcef-Toumi K, Ito O. A time delay controller for systems with unknown dynamics. J Dyn Syst Meas Cont 1990;112(1):133–42.
[28] Lin CJ, Yang SR. Precise positioning of piezo-actuated stages using hysteresis-observer based control. Mechatronics 2006;16(7):417–26.
[29] Lee J, Lee D, Won S. Precise tracking control of piezo actuator using sliding mode control with feedforward compensation. In: Proceedings of SICE Annual Conference 2010; 2010. p. 1244–9.
[30] Chang PH, Park SH. On improving time-delay control under certain hard nonlinearities. Mechatronics 2003;13(4):393–412.
[31] Cho GR, Chang PH, Park SH, Jin M. Robust tracking under nonlinear friction using time-delay control with internal model. IEEE Trans Control Syst Technol 2009;17(6):1406–14.
[32] Franklin G, Workman M, Powell D. Digital control of dynamic systems. Addison-Wesley Longman Publishing Co., Inc.; 1997.
[33] Pons J, Reynaerts D, Peirs J, Ceres R, VanBrussel H. Comparison of different control approaches to drive sma actuators. In: Proceedings of the 8th International Conference on Advanced Robotics, 1997. ICAR '97; 1997. p. 819–24.
[34] Mukherjee R, Minor M, Song G, Satava R. Optimisation of an articulated instrument for enhanced dexterity in minimally invasive therapy. Minim Invas Therapy All Technol 1998;7(4):335–42.
[35] Lee D, Allan J, Thompson HA, Bennett S. Pid control for a distributed system with a smart actuator. Control Eng Practice 2001;9(11):1235–44.
[36] Indiveri G. Swedish wheeled omnidirectional mobile robots: kinematics analysis and control. IEEE Trans Robot 2009;25(1):164–71.
[37] Kong K, Kniep HC, Tomizuka M. Output saturation in electric motor systems: Identification and controller design. J Dyn Syst Meas Control 2010;132(5):051002.
[38] Youcef-Toumi K, Wu S. Input/output linearization using time delay control. J Dyn Syst Meas Control 1992;114(1):10–9.
[39] Jung S, Hsia T, Bonitz R. Force tracking impedance control of robot manipulators under unknown environment. IEEE Trans Control Syst Technol 2004;12(3):474–83.
[40] Jin M, Kang SH, Chang PH. Robust compliant motion control of robot with nonlinear friction using time-delay estimation. IEEE Trans Ind Electron 2008;55(1):258–69.
[41] Wang W, Liu X. Fuzzy sliding mode control for a class of piezoelectric system with a sliding mode state estimator. Mechatronics 2010;20(6):712–9.
[42] Hughes D, Wen J. Preisach modeling of piezoceramic and shape memory alloy hysteresis. Smart Mater Struct 1997;6(3):287–300.
[43] Mayergoyz I. Mathematical models of hysteresis and their applications. Academic Press; 2003.
[44] Logemann H, Ryan E, Shvartsman I. A class of differential-delay systems with hysteresis: asymptotic behaviour of solutions. Nonlinear Anal: Theory, Meth Appl 2008;69(1):363–91.
[45] Su W, Drakunov S, Ozguner U. An o (t2) boundary layer in sliding mode for sampled-data systems. Automat Control, IEEE Trans 2000;45(3):482–5.
[46] Khalil H. Nonlinear systems. 3rd ed. Prentice Hall, Inc.; 2002.

Please cite this article in press as: Lee J et al. Precise tracking control of shape memory alloy actuator systems using hyperbolic tangential sliding mode control with time delay estimation. Mechatronics (2013), http://dx.doi.org/10.1016/j.mechatronics.2013.01.005